

# Deep Reinforcement Learning for Practical Phase Shift Optimization in RIS-aided MISO URLLC Systems

Ramin Hashemi, *Student Member, IEEE*, Samad Ali, *Member, IEEE*, Nurul Huda  
Mahmood, *Member, IEEE*, and Matti Latva-aho, *Senior Member, IEEE*

## Abstract

Industrial factory automation environments with multiple actuators and robots will benefit from reliable and low-latency wireless communication links to realize the key performance indicators (KPIs) defined in Industry 4.0 applications. Toward this goal, reconfigurable intelligent surfaces (RISs) can assist the wireless systems in providing such links. In this paper, the practical phase shift assignment in a RIS-aided ultra-reliable and low-latency communication (URLLC) system in a factory setting is studied. The optimization of phase shifts at the RIS elements is performed by applying a novel deep reinforcement learning (DRL) algorithm named as twin-delayed deep deterministic policy gradient (TD3). First, the system signal-to-interference-plus-noise ratio (SINR) and achievable rate in finite blocklength (FBL) regime are identified for each actuator in terms of the phase shift configuration matrix at the RIS. Then, the problem framework is proposed where the objective is to maximize the total achievable FBL rate in all actuators, subject to non-linear amplitude response and the phase shift constraint at the RIS elements. Since the amplitude response equality constraint is highly non-convex and non-linear, we resort to employing an actor-critic policy gradient DRL algorithm based on TD3. The considered method relies on interacting RIS with industrial automation environment by taking actions which are the phase shifts at the RIS elements, to maximize the expected observed reward, which is defined as the total FBL rate. We assess the performance loss of the system when the RIS is non-ideal, i.e., non-linear amplitude response with/without quantization of the phase shifts and compare it with ideal RIS in which the amplitude response is constant in terms of phase change. The numerical results show that optimizing the phase shifts in a non-ideal RIS via the proposed TD3 method is highly beneficial to improve the

The authors are with the Centre for Wireless Communications (CWC), University of Oulu, 90014 Oulu, Finland. e-mails: ({ramin.hashemi, samad.ali, nurulhuda.mahmood, matti.latva-aho}@oulu.fi).

This research has been financially supported by Academy of Finland 6Genesis Flagship (grant 318927).

network total FBL rate and it can lead to two-fold improvement in the total rate when the RIS phase shifts are optimized in comparison with random shift setting.

### Index Terms

Block error probability, deep reinforcement learning (DRL), finite blocklength (FBL), industrial automation, Industry 4.0, practical phase shift, reconfigurable intelligent surface (RIS), twin delayed DDPG (TD3), ultra-reliable low-latency communications (URLLC).

## I. INTRODUCTION

Industrial wireless systems involving devices, actuators and robots that require ultra-reliable and low-latency communications (URLLC) is anticipated to grow in the future sixth generation of wireless communications (6G) [1]. Industrial Internet of things (IIoT) is the industrial application of IoT connectivity along with networking and cloud computing based on data analytic collected from IoT devices. The industrial environments are very diverse and heterogeneous as they are characterized by a large number of use-cases and applications. An underlying commonality among these diverse applications is that the wireless industrial automation connectivity solutions envisioned in Industry 4.0 (initialized in 5G) [2] will leverage cloud computing and machine learning throughout the manufacturing process. The expected URLLC key performance indicators (KPIs) in 6G networks are *reliability* in the order of  $1 - 10^{-9}$ , *latency* around  $0.1 \sim 1$  ms round-trip time and *jitter* in the order of  $1 \mu s$  for industrial control networks [1]. There is also high data rate demand due to increased number of sensors and their resolution, e.g., for robots. In URLLC both the data and meta data sizes are small while both parts need to be very robust and have minimal error [3]. Thus, joint encoding of data and meta data is beneficial in terms of coding gain [4]. In addition, as the packet lengths in URLLC are usually small, the finite blocklength (FBL) theory is leveraged to investigate the penalty term in the achievable rate due to coding in FBL regime [5].

Recently, reconfigurable intelligent surface (RIS) has been introduced as a promising technology to enhance the energy efficiency, and spectral efficiency of wireless communications [6]. An RIS is composed of meta-materials where the phase and amplitude of each element can be adjusted. This allows the reflected signal to have a desired effect, e.g., enhance the received signal-to-interference-plus-noise ratio (SINR) at a given location. Because of this feature, the distribution of the received signal, when only the reflected channel through the RIS is available

due to blockage in the presence of obstacles, will be as deterministic as possible. Also, the performance of such systems depend on the quantization levels at each phase shift element or circuitry impairments [7], [8]. Thus, the application of the RIS technology in industrial automation in ensuring high reliability is very promising. Furthermore, since there is no processing overhead at the RIS and the increase in the delay spread caused by an RIS is rather small, unlike the conventional relays, the URLLC latency requirements can be satisfied as well by a suitable design in higher layer as the propagation delay along with the processing delay is negligible through the channel with RIS. Therefore, the RIS technology is highly beneficial in URLLC applications.

The fast and low-cost deployment characteristics in RIS technology make it more feasible in future industry and practical use cases in industrial automation. However, efficient physical layer design techniques, e.g., channel estimation, phase shift and amplitude response control and system-level optimizations, are still challenging and considered as active research topics. Toward this goal, optimization-oriented approaches relying on exhaustive alternating optimization methods or other solution frameworks have been leveraged throughout the literature in wide sense. Nevertheless, due to the unit modulus phase shifting constraint, the associated optimizations in the existing literature are highly non-convex and non-linear [9]. Thus, achieving a sub-optimal phase shift design is highly complicated and time-consuming. On the other side, while the radio channel characteristics vary over time or frequency, the optimization-based methods need to be re-executed to find the optimized phase shift values at the RIS which is impractical in mission-critical and sensitive industrial automation scenarios. Furthermore, the complexity of phase shift design optimizations increases when the practical RIS in which the amplitude response changes by the value of phase shift in a non-linear manner [10]. This poses new challenges to the existing optimization-based approaches which are still sophisticated and hard to solve even for ideal RISs.

In recent years, machine learning methods, particularly deep reinforcement learning (DRL) algorithms, have been considered as a reliable and powerful framework in wireless communications [11]. The DRL methods rely on taking action and receiving a certain reward based on the action and interacting with the environment, which constructs the agent's experience. Thus, these methods usually do not require large training data set, which is highly beneficial in practical resource allocation problems in wireless communications. Therefore, the applicability of DRL toward more reliable and faster solutions in the next generations of URLLC is highlighted with the advent of efficient new algorithms [11]–[13]. In this paper, our aim is to investigate

practical phase shift design and optimization of a RIS-assisted URLLC system in an industrial automation by employing a novel and sophisticated DRL algorithm named as twin delayed deep deterministic policy gradient (TD3). The total FBL achievable rate is considered as the objective to be maximized which highlights the performance reduction due to working in finite channel blocklength while ensuring an error probability as the target. Our proposed algorithm has several advantages over existing works, e.g., it is adaptive to channel state information (CSI) variations that occur in practical wireless systems and considers the impact of practical phase shifters at the RIS.

### A. Related Work

The resource allocation problems in URLLC systems over short packet communications with the assistance of the RIS technology is a relatively new topic and have only been investigated in a few papers [14]–[18]. In [14] the authors proposed an optimization problem for beamforming and phase shift control in a RIS-enabled orthogonal frequency division multiple access (OFDMA) URLLC systems where the cooperation of a set of base stations (BSs) to serve the URLLC traffic was studied. In [15] the unmanned aerial vehicles (UAVs) trajectory and channel blocklength as well as phase shift optimization in a RIS-aided network to minimize the total error probability is investigated. The considered system model is a RIS-aided URLLC system facilitated by a mobile UAV acting as a relay where the ground user receives short packets operating in FBL regime. In [16] the user grouping, channel blocklength and the reflective beamforming optimization in a URLLC system is studied where a dedicated RIS assists the BS in transmitting short packets in FBL scenario. The proposed optimization problem is tackled by well-known semi-definite relaxation (SDR) methods and the user grouping problem is solved by a greedy algorithm. The authors in [17], [18] studied the applicability of the RIS in joint multiplexing of enhanced mobile broadband (eMBB) and URLLC traffic to optimize the admitted URLLC packets while minimizing the eMBB rate loss to ensure the quality of service of the two traffic types by designing RIS phase shift matrices. Despite the interesting results in the aforementioned works, the use of highly sophisticated optimization-based algorithms is impractical as they usually rely on iterative algorithms with full CSI. Moreover, the non-linear amplitude response at the RIS elements breaks the structure of most optimization-based algorithms when it is taken into account. Particularly, even with an appropriate method that considers such constraint, the computational complexity of such algorithms is still unsatisfactory. Therefore, the low-complexity phase shift

design at the practical RIS is of paramount importance in URLLC systems operating in FBL regime.

In recent years the development of machine learning algorithms, especially DRL approaches in phase shift design at the RIS has gained significant interest [19]–[35]. In [19] the secrecy rate of a wireless channel with RIS technology is maximized with quality of service (QoS) constraints on the secrecy rate and data rate requirements of the users in which the transmit beamforming vectors and the RIS phase shifts are the design variables. The resulting problem is solved by a novel DRL algorithm that improves the learning efficiency of the policy gradient algorithm by employing post-decision state and prioritized experience replay methods. The authors in [20] considered a downlink multiple-input single-output (MISO) system to adjust the RIS phase shifts as well as the coordinate of the flying UAV and transmit power via a decaying deep Q network (DQN) algorithm. A novel actor-critic DRL algorithm named as deep deterministic policy gradient (DDPG) that is a model-free and off-policy method for learning continuous actions is employed in [21] to maximize the secrecy rate in a downlink MISO system via adjusting the phase shifts at the RIS. In [22], the half-duplex and full-duplex operating modes are discussed and compared in a RIS-aided MISO system and a reflective phase shift design problem of the RIS elements is proposed via DDPG method. The work in [23] investigated the RIS phase shift optimization in a problem of joint relay selection and RIS reflection coefficient optimization. In addition, in [24], [25] the problem of maximizing the total achievable rate in infinite blocklength regime in multi-hop multi-user RIS-aided wireless terahertz (THz) communication system was studied. The authors in [26] investigated the applicability of the DDPG method in a RIS-assisted MISO system to adjust the transmit beamforming vector and the RIS phase shift. The objective of the considered problem is the total achievable rate in infinite blocklength regime across the network subject to unit modulus phase shift constraints, i.e., considering ideal RIS with continuous phase shift and the maximum transmit power of the BS.

In [27] the DRL algorithm based on DQN in providing energy-efficient and robustness against channel uncertainty via RIS reflective design is studied. The combination of model-free and model-based DRL algorithms is studied in [28] where the learning performance is improved by proposing a novel optimization-driven DDPG approach to optimize the RIS phase shift elements' values. The application of DDPG method in non-orthogonal multiple access (NOMA) networks employing RIS technology is also investigated in [29], [30]. A comparison between DRL methods with optimization-based algorithms in RIS phase shift allocation is studied in [31]. The perfor-

mance of an anti-jamming wireless system is shown to be enhanced by the use of RIS in [32]. The authors showed that fuzzy win or learn fast-policy hill-climbing (WoLF-CPHC) learning approach achieves the optimal anti-jamming strategy through transmit power and reflective phase shift values as the agent's action space. The maximization of the mmWave secrecy rate by jointly optimizing the UAV trajectory, beamforming vectors and RIS phase shift is conducted in [33] where two independent DDPG networks, i.e., twin DDPG are leveraged to allocate the action strategies. The channels' feedback delay which results in channel coefficients' obsolescence, is also taken into account and the performance loss due to this effect is assessed. In [34], the DDPG algorithm was employed to optimize the power and the reflective surface phase shift design in a multi-UAV-enabled network while the authors in [35] analyzed the application of DDPG algorithm in UAV trajectory, power control and RIS phase shift optimization in a NOMA network. In Table I, we have summarized the aforementioned recent studies on RIS phase shift configuration based on DRL algorithms.

### *B. Contributions*

Despite the interesting results in the aforementioned works on the reflective phase shift design in RIS-aided communications, the impact of impairments in practical RIS with non-linear amplitude response on the performance of a URLLC system over FBL regime has not been investigated before. In addition, most of the prior studies assumed that the RIS is ideal and the scenario is infinite blocklength regime. Also, as mentioned before, the majority of the existing literature employed the conventional DDPG algorithm to solve the proposed resource allocation problem. Nevertheless, there are drawbacks associated with this method which are addressed in the novel twin-delayed DDPG, i.e., TD3 method [36]. Firstly, the action-value function is overestimated which is handled by introducing two deep neural networks (DNNs) and selecting the minimum of each output. Secondly, the target and the policy networks are being updated less frequently than the critic networks to avoid unexpected actions and sudden performance degradation that results in enhancing the learning efficiency. Thirdly, regularization of the actions is performed that may cause failure to the action-value function of the next states in DDPG. Therefore, applying this method in non-ideal RIS phase shift design over short packet communication systems is advantageous to ensure the stability of the performance. More specifically, motivated by the compelling works on resource allocation via DRL methods in RIS communications, we aim to elaborate the phase shift control problem where the objective is to

TABLE I: A summary of contributions of the existing works (IL: interference-limited, i.e., considering SINR, IF: interference-free, i.e., considering SNR).

Feature Ref.	System model	RL method	State	Action	Discrete phase
[19]	DL MISO, IL	Deep PDS-PER	CSI, last slot rate, QoS satisfaction level	Beamforming, RIS phase config.	–
[20]	DL MISO, IL	Decaying-DQN	RIS phase, coordinate of the UAV and users, transmit power	RIS phase shift, traveling direction, power change	✓
[21]	DL MISO, IF	DDPG	Last slot SNR, RIS phases	RIS phase config.	–
[22]	DL MISO, IL	DDPG	Last slot rate, RIS phases	RIS phase config.	–
[23]	SISO hybrid relay-RIS	Double DQN	CSI, time slot	RIS phase config.	✓
[24], [25]	Multi-hop RIS MISO, IL	DDPG	CSI, beamforming and RIS phase config. matrix	Beamforming and RIS phase config.	–
[26]	MISO, IL	DDPG	CSI, last slot action, beamforming matrix	RIS phase config. and beamforming matrix	–
[27]	DL MISO, IL	DQN	Beamforming vectors, energy level of RIS	RIS phase config., element ON/OFF state and transmit power	✓
[28]	MISO, IF	Optimization-driven DDPG	CSI, outage indicator (constraint satisfaction)	Beamforming vector, RIS phase config.	–
[29]	DL MISO NOMA, IL	DDPG	RIS phase matrix	RIS phase matrix change	✓
[30]	DL NOMA, IL	DDPG	CSI, phase config. matrix, last slot SINR	RIS phase config.	–
[32]	DL MISO, IL	Fuzzy win or learn fast-policy hill-climbing (WoLF-CPHC)	CSI, phase config. matrix, last slot SINR, transmit power	Transmit power, RIS phase config.	–
[33]	DL MISO, IL	Double DDPG	Online CSI	Phase config. matrix, beamforming vectors and UAV trajectory	–
[34]	DL SISO, IL	DDPG	Effective CSI	Transmit power and the phase config. matrix	–
[35]	DL SISO NOMA, IL	DDPG	Last slot rates, phase config. matrix, UAV trajectory and power allocation coefficient	Transmit power, the phase config. matrix and UAV trajectory	–

maximize the total FBL rate in an industrial automation scenario with multiple actuators subject to non-linear amplitude response and discrete phase shift constraints. Moreover, the proposed DRL algorithm is robust to channel variations over different time-slots due to being outdated because of feedback delay which deteriorates the performance. The contributions of our work are summarized in the following:

- A multi-antenna BS serving multiple actuators in the presence of a practical RIS is considered in industrial automation. The RIS imperfections are modeled based on the empirical amplitude response in terms of phase shift values and the quantization of continuous phase

shifts. Additionally, the radio channels' response where the coefficients become outdated due to feedback delay is characterized. The total FBL rate in downlink with minimum mean square error (MMSE) receiver, subject to a target block error probability (BLER), is considered as the system performance indicator over short packet communications. Based on the proposed system model, the reflective phase shift optimization is formulated in which the objective is to maximize the total FBL rate of all actuators subject to discrete phase shift constraints and non-linear amplitude responses at the RIS elements.

- Since the formulated problem is highly non-linear and non-convex, we invoke a novel policy gradient actor-critic DRL algorithm to solve the problem. Specifically, we leverage TD3 method in which recruits two additional DNNs to reduce the estimation error of action-values and updates the main policy network less frequently than critic networks to stop overestimation of the action-value function, which usually leads to the policy breaking.
- The numerical results show that while the TD3 algorithm is well-suited to the proposed problem compared to typical DDPG scheme, it is essential to optimize phase shifts at the practical RIS with impairments to enhance the network total FBL rate. Furthermore, the performance reduction gap between an ideal RIS with continuous phase shift and the non-ideal RIS with discrete phase shifts is elaborated. The results show that properly optimizing the phase shifts while considering non-linear amplitude response with/without discrete phase shifts at the elements of the RIS, the total FBL rate will improve significantly.

### C. Notations and Structure of the Paper

In this paper,  $\mathbf{h} \sim \mathcal{CN}(\mathbf{0}_{N \times 1}, \mathbf{C}_{N \times N})$  denotes a  $N$ -dimensional circularly-symmetric (central) complex normal distribution vector with zero mean vector  $\mathbf{0}_{N \times 1}$  and covariance matrix  $\mathbf{C}$ . The operations  $[\cdot]^H$ ,  $[\cdot]^T$  denote the transpose and conjugate transpose of a matrix or vector, respectively.

The structure of this paper is organized as follows. In Section II, the system model and the FBL rate is proposed, then the optimization framework of phase shift design at the RIS is presented. In Section III the DRL preliminaries and exploited solution approach is studied. The numerical results are presented in Section IV. Finally, Section V concludes the paper.

## II. SYSTEM MODEL AND PROBLEM FORMULATION

### A. System Model

Consider the downlink (DL) of an RIS-assisted wireless network in a factory setting which consists of a BS with  $M = M_x \times M_y$  uniform planar array (UPA) antennas and  $K$  actuators. The RIS which has  $N = N_x \times N_y$  phase shift elements constructs a line-of-sight (LoS) channel between itself the actuators and multi-antenna BS. However, the direct channel between the BS and actuators is covered by possible blockages in the factory and only non-LoS (NLoS) channel exists. The total channel response between the BS and an actuator has a direct path component plus a reflected path from the RIS as illustrated in Fig. 1. The channel matrix between BS and the RIS is denoted as

$$\mathbf{H} = \bar{\mathbf{H}}_{\text{LoS}} + \mathbf{H}_{\text{NLoS}} = [\mathbf{h}_1^{\text{inc}}, \dots, \mathbf{h}_M^{\text{inc}}] \in \mathbb{C}^{N \times M}, \quad (1)$$

where the column vector  $\mathbf{h}_m^{\text{inc}} = \frac{\zeta}{\zeta+1} \bar{\mathbf{h}}_m^{\text{inc}} + \frac{1}{\zeta+1} \tilde{\mathbf{h}}_m^{\text{inc}}$  for  $\forall m \in \{1, \dots, M\}$  where  $\tilde{\mathbf{h}}_m^{\text{inc}} \sim \mathcal{CN}(\mathbf{0}_{M \times 1}, \boldsymbol{\beta}^{\text{inc}})$ ,  $\boldsymbol{\beta}^{\text{inc}} = \text{diag}(\beta_1^{\text{inc}}, \dots, \beta_M^{\text{inc}})$  denotes the covariance matrix of NLoS path containing the pathloss coefficients from BS to the RIS. Additionally, the LoS channel  $\bar{\mathbf{H}}_{\text{LoS}}$  is defined as [37]

$$\bar{\mathbf{H}}_{\text{LoS}} = \mathbf{a}^{\text{H}}(\phi_1^a, \phi_1^e, N_x, N_y) \times \mathbf{a}(\phi_2^a, \phi_2^e, M_x, M_y), \quad (2)$$

where  $\phi_1^{a/e}$  denote the azimuth (elevation) angle of a row (column) of the UPA at the RIS and the projection of the transmit signal from BS to the RIS on the plane of the UPA at the RIS. Similarly,  $\phi_2^{a/e}$  shows the azimuth (elevation) angle between the direction of a row (column) of the UPA at BS and the projection of the signal from BS to the RIS on the plane of the UPA at BS. In addition [37]

$$\mathbf{a}(\phi^a, \phi^e, N_1, N_2) := \text{rvec} \left( \left( e^{j\mathcal{G}(x,y,n_1,n_2)} \right)_{n_1=1,2,\dots,N_1, n_2=1,2,\dots,N_2} \right), \quad (3)$$

where  $\text{rvec}(\cdot)$  denotes the row vectorization of a matrix and

$$\mathcal{G}(x, y, n_1, n_2) = 2\pi \frac{d}{\lambda} [(n_1 - 1) \cos x + (n_2 - 1) \sin x] \sin y, \quad (4)$$

in which  $\lambda$  is the operating wavelength, and  $d$  is the antenna/element spacing. Similarly, the channel between RIS and actuator  $k$  is

$$\mathbf{h}_k^{\text{RIS}} = \frac{\zeta_k^{\text{RIS}}}{\zeta_k^{\text{RIS}} + 1} \bar{\mathbf{h}}_k^{\text{RIS}} + \frac{1}{\zeta_k^{\text{RIS}} + 1} \tilde{\mathbf{h}}_k^{\text{RIS}}, \quad (5)$$

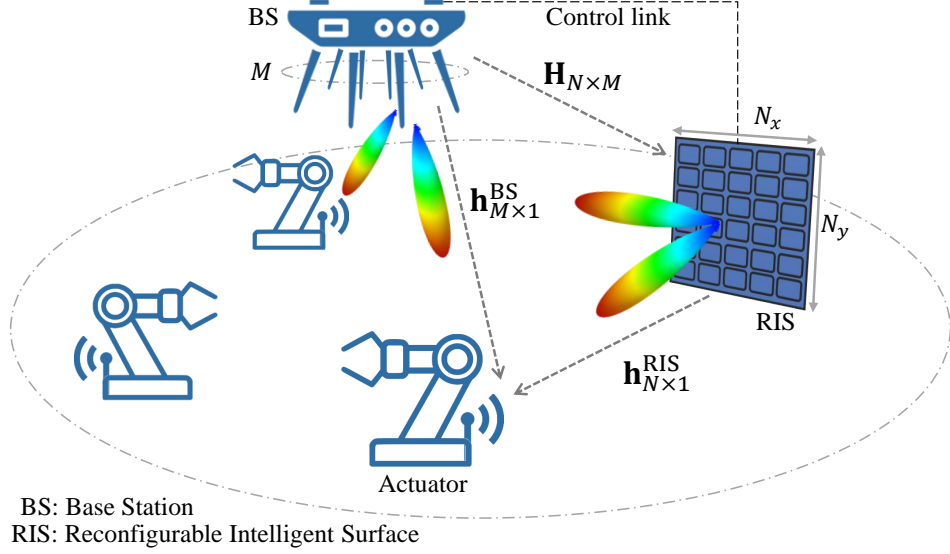


Fig. 1: The considered system model.

where the Rician parameter  $\zeta_k^{\text{RIS}}$  controls the proportion of LoS to the none-LoS power in actuator  $k$ . The NLoS channel is distributed as  $\tilde{\mathbf{h}}_k^{\text{RIS}} \sim \mathcal{CN}(\mathbf{0}_{N \times 1}, \boldsymbol{\beta}_k^{\text{RIS}})$  and  $\boldsymbol{\beta}_k^{\text{RIS}} = \text{diag}(\beta_1^{\text{RIS}_k}, \dots, \beta_N^{\text{RIS}_k})$  is the covariance matrix containing the pathloss coefficients from RIS to actuator  $k$ . Furthermore, the LoS channel  $\bar{\mathbf{h}}_k^{\text{RIS}} \in \mathbb{C}^{N \times 1}$  is modeled by

$$\bar{\mathbf{h}}_k^{\text{RIS}} = \mathbf{a}(\phi_3^a, \phi_3^e, N_x, N_y), \quad \forall k \in \{1, 2, \dots, K\}, \quad (6)$$

in which  $\phi_3^a, \phi_3^e$  are the azimuth/elevation angles between RIS and the actuator  $k$ . The direct path between BS and the actuators are blocked and only the NLoS channel exists as  $\mathbf{h}_k^{\text{BS}} \sim \mathcal{CN}(\mathbf{0}_{M \times 1}, \boldsymbol{\beta}_k^{\text{BS}}) \in \mathbb{C}^{M \times 1}$  and  $\boldsymbol{\beta}_k^{\text{BS}} = \text{diag}(\beta_1^{\text{BS}_k}, \dots, \beta_M^{\text{BS}_k})$ .

In this work we assume single-shot transmissions, i.e., retransmissions are not considered [38], [39]. Thus, the transmission latency is equal to one transmission time interval, which can be as low as  $\sim 0.1$  ms when adopting the flexible numerology introduced in 5G New Radio [40]. This assumption allows us to investigate the lower-bound performance of the proposed URLLC system as retransmissions improve the reliability of the system while at the cost of increasing latency [41]. Nevertheless, some studies have compared the retransmission schemes with single-shot transmission [39], [42]. As an example, the study in [42] employed incremental redundancy hybrid automatic repeat request (IR-HARQ) and concluded that the energy saving of the system enhances in comparison with single-shot transmission. For the considered system

model, the received signal at the actuator  $k$  is

$$y_k[t] = \overbrace{\left(\mathbf{h}_k^{\text{BSH}} + \mathbf{h}_k^{\text{RISH}} \Theta \mathbf{H}\right) \mathbf{s}_k[t] x_k}^{\text{Actuator } k \text{ signal}} + \overbrace{\left(\mathbf{h}_k^{\text{BSH}} + \mathbf{h}_k^{\text{RISH}} \Theta \mathbf{H}\right) \sum_{i=1, i \neq k}^K \mathbf{s}_i[t] x_i + n_k[t]}^{\text{Interference plus noise}}, \quad (7)$$

where  $\mathbf{s}_k[t]$  is the beamforming vector applied at the transmitter to the symbol  $x_k \sim \mathcal{CN}(0, 1)$  of actuator  $k$  with  $\|\mathbf{s}_k[t]\|^2 = p_k$  in which  $p_k$  is the transmit power allocated for actuator  $k$  such that  $\sum_{k=1}^K p_k = p_{\text{total}}$  is the BS transmit power, and  $n_k[t]$  is the additive white Gaussian noise with  $\mathbb{E}[|n_k[t]|^2] = N_0 W = \sigma^2$  where  $N_0$ ,  $W$  are the noise spectral density and the system bandwidth, respectively. The complex reconfiguration matrix  $\Theta_{N \times N}$  indicates the phase shift setting of the RIS which is defined as

$$\Theta_{N \times N} = \text{diag}(\beta_1 e^{j\theta_1}, \beta_2 e^{j\theta_2}, \dots, \beta_N e^{j\theta_N}),$$

$$\beta_n \in [0, 1], \quad \theta_n \in [-\pi, \pi), \quad \forall n \in \mathcal{N} \quad (8)$$

where  $\mathcal{N} = \{1, 2, \dots, N\}$ . Note that in our model we have assumed that the RIS elements have no coupling or there is no joint processing among elements [6]. However, practical RIS phase shifters have phase-dependent amplitude response which is given by [10]

$$\beta_n(\theta_n) = (1 - \beta_{\min}) \left( \frac{\sin(\theta_n - \phi) + 1}{2} \right)^\alpha + \beta_{\min}, \quad (9)$$

where  $\beta_{\min} \geq 0$  (minimum amplitude),  $\alpha \geq 0$  (the steepness) and  $\phi \geq 0$  (the horizontal distance between  $-\frac{\pi}{2}$  and  $\beta_{\min}$ ) are circuit implementation parameters. Note that,  $\beta_{\min} = 1$  results in an ideal phase shifter. Furthermore, without considering hardware impairments at the RIS the optimal phase of the RIS is picked up from [9]

$$\Upsilon(\theta_n) = \hat{\theta}_n \in \Phi = \{-\pi, -\pi + \Delta, -\pi + 2\Delta, \dots, -\pi + (Q - 1)\Delta\}, \quad \forall n \in \mathcal{N} \quad (10)$$

where  $\Upsilon(\cdot)$  denotes the quantizer system response and  $Q = 2^b$  is the number of quantization levels,  $b$  denotes the number of bits assigned to a discrete and quantized phase and  $\Delta = \frac{\pi}{2^{b-1}}$  is the quantization step. Through this process, a phase error  $e$  distributed uniformly over  $-\frac{\Delta}{2} \leq e \leq \frac{\Delta}{2}$  appears which deteriorates the system performance. Let us denote the phase error as  $\phi_n \sim \mathcal{U}(-\kappa\pi, \kappa\pi)$ ,  $\forall n \in \mathcal{N}$  where  $\kappa = \frac{1}{2^b} \in (0, 1]$ .

Therefore, based on the received signal at actuator  $k$  the MMSE signal detection is performed

to extract the transmitted symbols. Henceforth, the SINR will be

$$\text{SINR}_k(\Theta) = p_k \mathbf{h}_k^H(t) \left( \sigma^2 \mathbf{I}_M + \sum_{i=1, i \neq k}^K p_i \mathbf{h}_i(t) \mathbf{h}_i^H(t) \right)^{-1} \mathbf{h}_k(t), \quad (11)$$

where  $\mathbf{h}_k(t) = \mathbf{h}_k^{\text{BS}}(t) + \mathbf{H}^H(t) \Theta^H(t) \mathbf{h}_k^{\text{RIS}}(t)$  and  $\Theta(t) \in \mathbb{C}^{N \times N}$  denotes the reconfiguration phase matrix and  $t$  is the time instance index.

In practice, the channel estimates become outdated after a delay time  $T_d$  which results in imperfect CSI. To model the channel variations, delayed feedback is expressed as [43]

$$\mathbf{h}_k(t) = \rho_d \mathbf{h}_k(t - T_d) + \mathbf{e}_k(t), \quad (12)$$

where  $T_d$  is the feedback delay,  $\mathbf{e}_k(t) \sim \mathcal{CN}(\mathbf{0}, \sqrt{1 - \rho_d^2} \mathbf{I}_M)$  and

$$\rho_d = \frac{\mathbb{E}[\mathbf{h}_k^H(t) \mathbf{h}_k(t - T_d)]}{\mathbb{E}[\mathbf{h}_k^H(t) \mathbf{h}_k(t)]}, \quad (13)$$

is the normalized correlation coefficient between the current and the outdated channel response. According to Clarke's fading spectrum model for band-limited channels  $\rho_d = J_0(2\pi T_s f_d T_d)$  where  $J_0(\cdot)$  is the zeroth order of the Bessel function of the first kind,  $f_d$  is Doppler frequency and  $T_s$  is the symbol block duration. Note that  $\rho_d = 1$  corresponds to perfect channel updates which may be impractical due to channel variations over time. In this paper, we assume that the channel coefficients are varying over time so that at time  $t$ , only the channel responses which are delayed with  $T_d$  are available at the BS.

Based on the received SINR at actuator  $k$  the number of information bits that can be transmitted through  $m_k$  channel uses over a quasi-static additive white Gaussian channel (AWGN) is given by [5]

$$L_k = m_k C(\text{SINR}_k) - \mathcal{Q}^{-1}(\varepsilon_k) \sqrt{m_k V(\text{SINR}_k)} + \mathcal{O}(\log_2(m_k)), \quad (14)$$

where  $C(\text{SINR}) = \log_2(1 + \text{SINR})$  is the Shannon capacity which is defined in infinite blocklength regime and  $\varepsilon_k$  is the target error probability for actuator  $k$  while  $\mathcal{Q}^{-1}(\cdot)$  is the inverse of  $\mathcal{Q}$ -function defined as  $\mathcal{Q}(x) = \frac{1}{\sqrt{2\pi}} \int_x^\infty e^{-\nu^2/2} d\nu$ . The channel dispersion is defined as

$$V(\text{SINR}_k) = \frac{1}{(\ln 2)^2} \left( 1 - \frac{1}{(1 + \text{SINR}_k)^2} \right), \quad (15)$$

By solving (14) in order to find the decoding error probability  $\varepsilon_k$  at the actuator  $k$  it yields

$$\varepsilon_k = \mathcal{Q}(f(\text{SINR}_k, m_k, L_k)), \quad (16)$$

where

$$f(\text{SINR}_k, m_k, L_k) = \sqrt{\frac{m_k}{V(\text{SINR}_k)}} \left( \log_2(1 + \text{SINR}_k) - \frac{L}{m_k} \right), \quad (17)$$

Also, note that from (14) when the blocklength  $m_k$  asymptotically goes infinity the achievable rate will be simplified to

$$\lim_{m_k \rightarrow \infty} \frac{L(m_k, p_k, \varepsilon_k)}{m_k} = \log_2(1 + \text{SINR}_k), \quad (18)$$

which is the conventional Shannon capacity formula.

### B. Problem Formulation

Optimizing the total FBL rate of the actuators to ensure the transmission target error probability by configuring the phase matrix of the RIS is essential in factory environments. Toward this, we formulate the following optimization problem (OP):

$$\begin{aligned} \mathbf{P1} \quad & \max_{\Theta} L_{\text{tot}}(\Theta) = \sum_{k=1}^K [\mathcal{V}_k(\Theta) - \mathcal{Q}^{-1}(\varepsilon_k^{\text{th}}) \mathcal{W}_k(\Theta)] \\ \text{s.t.} \quad & \mathbf{C}_1: \theta_n \in \Phi, \quad \forall n \in \mathcal{N}, \\ & \mathbf{C}_2: \beta_n(\theta_n) = (1 - \beta_{\min}) \left( \frac{\sin(\theta_n - \phi) + 1}{2} \right)^\alpha + \beta_{\min}, \quad \forall n \in \mathcal{N}, \end{aligned} \quad (19)$$

where  $\mathcal{V}_k(\Theta) = m_k \mathbf{C}(\text{SINR}_k)$ ,  $\mathcal{W}_k(\Theta) = \sqrt{m_k \mathbf{V}(\text{SINR}_k)}$ , the objective is to maximize the total number of information bits across all actuators and the variables are the reflective phase shift values of each element in  $\Theta$  at the RIS. The aim of transmission in the FBL regime is to ensure the BLER at a target value which is equal to  $\varepsilon_k^{\text{th}} \forall k \in \{1, 2, \dots, K\}$  in the objective function. Thus, by maximizing the objective in **P1** while transmitting with the specified FBL rate, the error probability will be ensured to target value as well. The constraint  $\mathbf{C}_1$  denotes that the phase adjustment variable is selected from the discrete set  $\Phi$  given in (10).  $\mathbf{C}_2$  implies the practical phase shift model which affects the amplitude response of the RIS.

It is observed from **P1** that it belongs to a class of mixed integer nonlinear combinatorial optimization problem which is thoroughly challenging to solve. On the other words, the RIS

phase shifts must be chosen from discrete set  $\Phi$ , where  $|\Phi| = Q$  is the number of possible phase values for each element. It is perceived that for an RIS with  $N$  elements there are  $Q^N$  possible realizations of phase configuration matrices of which optimized values are found either by exhaustive search or optimization algorithms. Even with  $Q = 2$  (as a simple 1-bit phase shifter), we will have a large state space  $\mathcal{O}(2^N)$  that is challenging to find the best phase shifts by employing exhaustive methods as the search space grows rapidly with the number of RIS elements and quantization levels. Therefore, we relax the constraint  $C_1$  to be continuous variables and use the following rule for discretizing the reflective phase shifts:

$$\hat{\theta}_n = \arg \min_{\theta \in \Phi} |\theta_n - \theta|, \quad (20)$$

Nevertheless, the problem is still non-linear due to equality constraint  $C_2$ . Thus, leveraging optimization-based solutions for the **P1** is also shown to be intractable due to the non-linear equality constraint  $C_2$  and non-convex objective function. Consequently, we resort to employing model-free DRL algorithm based on the TD3 algorithm which is presented in the following section.

### III. DRL-BASED FORMULATION

#### A. Review on the Preliminaries

The goal of the agent in reinforcement learning (RL) is to *learn* to find an optimal policy that maps states to actions based on its interaction with the environment so that the accumulated discounted reward function over a long time is maximized. A state contains all useful information from the sequence of the observations, actions and rewards. This kind of problems are tackled by representing them as Markov decision process (MDP) framework. An MDP is characterized by  $(\mathcal{S}, \mathcal{A}, \mathcal{R}, \mathcal{P}_{s \rightarrow s'})$  in which  $\mathcal{S}$  is the set of environment states,  $\mathcal{A}$  denotes the set of possible actions, which for this case is defined in terms of the RIS phase shift values,  $\mathcal{R}$  is the reward function, and  $\mathcal{P}_{s \rightarrow s'}$  is the transition probabilities from state  $s$  to  $s'$ ,  $\forall s, s' \in \mathcal{S}$ . Mathematically, a Markov property means that the probability of next state (future state) is independent of the past given the present state. In RL algorithms, the environment can be fully or partially observable. In a fully observable environment, the agent directly observes the environment [44]. The aim of the agent is to find an optimal policy to maximize the accumulated and discounted reward

function over time-steps, i.e., to find  $\pi^*$  in which the set of states  $\mathcal{S}$  is mapped into the set of actions  $\mathcal{A}$  as  $\pi^* : \mathcal{S} \rightarrow \mathcal{A}$ . The optimal policy  $\pi^*$  maximizes the action-value function defined as

$$Q_\pi(s, a) = \mathbb{E}_\pi \left[ \sum_{t=0}^{\infty} \gamma^t r_{t+k+1} | S_t = s, A_t = a \right], \quad (21)$$

where the variable  $0 \leq \gamma \leq 1$  is the discount factor to uncertainty of future rewards,  $r_i$  is the acquired reward in step  $i$  and  $\mathbb{E}_\pi[\cdot]$  denotes the expectation with respect to policy  $\pi$ . By invoking Markov property and Bellman equation, (21) will be reformulated into,

$$Q_\pi(s, a) = \mathbb{E}_\pi \left[ r_{t+1} + \gamma \sum_{a' \in \mathcal{A}} \pi(a'|s') Q_\pi(s', a') | S_t = s, A_t = a \right], \quad (22)$$

which  $\pi(a'|s')$  gives the probability of choosing action  $a'$  given that the agent is in state  $s'$ , the optimal value for action-value function can be achieved by [45]

$$Q_{\pi^*}(s, a) = \sum_{s' \in \mathcal{S}, r \in \mathcal{R}} \Pr(s'|s, a) \left( r + \gamma \max_{a'} Q_{\pi^*}(s', a') \right), \quad (23)$$

where  $\Pr(s'|s, a)$  is the probability of transition to state  $s'$  given that the agent is in state  $s$  and the taken action is  $a$ . In order to find the optimal policy in (23), one must have knowledge about the transition probabilities that are usually unknown due to the environment structure.

To find the optimal policy, two general methods can be leveraged. An RL problem can be solved using *model-based* methods, where the transition probabilities to the next state are given and reward function values are known. However, in most applications and specifically in our system model, the environment transition probabilities are unknown or even hard to find. Fortunately, thanks to *model-free* algorithms in RL problems, the agent can learn the optimal policy by interacting with the environment while receiving a reward. In model-free methods, a ground-truth model of the environment is not needed to be available at the agent. Moreover, they are tractable and straightforward to implement in comparison with model-based frameworks.

Q-learning is an example of model-free learning of the optimal policy which does not require to have knowledge about system parameters like state transition probabilities and the reward function before taking actions. However, the size of the state and action space must be small enough to efficiently achieve the optimal policy. Since for each action-space pair the Q-value, i.e., the action-value function must be evaluated and stored in the Q-table. The size of the Q-table is the product of the cardinality of action space by the size of state space, which is quite problematic in terms of required memory and computational complexity for large action or state

space problems. The same problem exists in deep Q-learning methods as they exploit a DNN to estimate the Q-value for each action-space pair. Furthermore, when a nonlinear estimator is used in deep Q-learning methods, the average reward might diverge or become unstable. To address the challenge, experience replay memory is introduced which trains the DNN based on the mini-batches of the stored experience in the buffer. A key insight to employ experience replay memory is to break the correlation between consecutive samples by taking random samples.

On the other hand, an RL problem can be solved by directly estimating the policy function rather than investigating the action-value function. These methods are named as policy-gradient (PG). In PG methods, the policy can be parameterized as a function of states on a DNN network. Let us denote the policy DNN with parameters' set  $\xi^{\text{act}}$  as

$$\pi(a|s; \xi^{\text{act}}) = \Pr(A = a | S = s; \xi^{\text{act}}), \quad (24)$$

where  $A = a$  is the action to be taken in state  $S = s$ . The probability of transiting to the state  $s'$  from  $s$  while taking action  $a$  is shown as  $\Pr(s'|s, a)$ . In PG methods the DNN weights are updated based on the result from policy-gradient theorem [45] which expresses that evaluating the gradient of the objective function given by

$$J(\xi^{\text{act}}) \triangleq \sum_{s \in \mathcal{S}} d^\pi(s) \sum_{a \in \mathcal{A}} \pi(a|s; \xi^{\text{act}}) Q(s, a; \xi^{\text{crit}}), \quad (25)$$

is independent of the stationary distribution for states denoted as  $d^\pi(s)$  for policy  $\pi(\cdot)$ . In (25),  $Q(s, a; \xi^{\text{crit}})$  represents the action-value function parameterized by  $\xi^{\text{crit}}$ . The actor-critic networks are temporal difference (TD) learning methods that represent the policy function independent of the action-value function. We aim to employ actor-critic method where the policy is referred to as the actor that proposes a set of possible actions on a state. In actor-critic methods another DNN is employed to estimate the the action-value function  $Q(s, a; \xi^{\text{crit}})$ . The DNN evaluates the action-value by importing the current state and the action given by the policy network and its weights are represented as  $\xi^{\text{crit}}$ .

One of the efficient model-free and off-policy actor-critic methods that deals with the continuous action-space is DDPG [46]. In this algorithm, four DNNs are employed, two of them are for actor-critic networks and the other two are called target networks. The actor network directly gives the action by importing the states through a DNN with parameter set  $\xi^{\text{act}}$ , i.e.,  $a = \mu(s; \xi^{\text{act}})$  where  $\mu(\cdot)$  denotes the deterministic policy meaning that the output is a value

instead of a distribution. The critic network that has a DNN with  $\xi^{\text{crit}}$  weights evaluates the action-value function based on the action given by the policy network and the current state. The other two networks which are named as target networks give the target action-values in order to minimize the mean-squared Bellman error (MSBE) which is defined as [44]

$$\text{Loss}(\xi^{\text{crit}}, \mathcal{B}) \triangleq \mathbb{E}_{(s,a,s',r) \sim \mathcal{B}} \left[ \left( Q(s, a; \xi^{\text{crit}}) - \overbrace{(r + \gamma \max_{a'} Q(s', a'; \xi^{\text{crit}}))}^{\text{target value}} \right)^2 \right], \quad (26)$$

where  $\mathcal{B}$  is the experience replay memory which has stored the set of states, actions, rewards and the next states as a tuple  $(s, a, r, s')$  over previous steps. From (26) the next optimal action  $a'$  is calculated by the target actor network with parameter set  $\xi^{\text{targ-act}}$  where  $a' = \mu(s'; \xi^{\text{targ-act}})$  and the corresponding action-value  $Q(s', a'; \xi^{\text{targ-crit}})$  is then evaluated using the target critic network with weights  $\xi^{\text{targ-crit}}$ . The two networks weights are usually just copied over from the main network every some-fixed-number of steps by polyak averaging which is

$$\xi^{\text{targ-act}} \leftarrow \tau \xi^{\text{act}} + (1 - \tau) \xi^{\text{targ-act}}, \quad (27)$$

$$\xi^{\text{targ-crit}} \leftarrow \tau \xi^{\text{crit}} + (1 - \tau) \xi^{\text{targ-crit}}, \quad (28)$$

where  $\tau \ll 1$  is the hyperparameter used to control the updating procedure.

### B. Twin Delayed DDPG (TD3)

Before proceeding with TD3 method, we restate the following Lemma from [36]:

**Lemma 1.** *For the true underlying action-value function which is not known during the learning process, i.e.,  $Q_\pi(s, a)$  and the estimated  $Q(s, a; \xi^{\text{crit}})$  the following inequality holds*

$$\mathbb{E} \left[ Q \left( s, a = \mu(s; \xi^{\text{act}}); \xi^{\text{crit}} \right) \right] \geq \mathbb{E} \left[ Q_\pi \left( s, a = \mu(s; \xi^{\text{act}}) \right) \right], \quad (29)$$

Based on Lemma 1, since the DDPG algorithm leverages the typical Q-learning methods, it overestimates the Q-values during the training which propagates throughout the next states and episodes. This effect deteriorates the policy network as it utilizes the Q-values to update its weights and hyperparameters and results in poor policy updates. The impact of this overestimation bias is even problematic with feedback loop that exists in DRL methods where suboptimal actions might be highly rated by biased suboptimal critic networks. Thus, the suboptimal actions will

be reinforced in next policy updates. The TD3 algorithm introduces the following assumptions to address the challenges [36]

- As illustrated in Fig. 2, TD3 recruits two DNNs for estimating the action-value function in the Bellman equation, then the minimum value of the output of Q-values is used in the (26).
- In this method, the target and policy networks are being updated less frequently than critic networks.
- A regularization of the actions that can incur high peaks and failure to the Q-value in DDPG method is leveraged so that the policy network will not try these actions in the next states. Therefore, the action will be chosen based on adding a small amount of clipped random noise to the selected action as given by

$$a' = \text{clip}(\mu(s'; \xi^{\text{targ-act}}) + \text{clip}(\kappa, -c, +c), a_{\text{Low}}, a_{\text{High}}), \quad \kappa \sim \mathcal{N}(0, \tilde{\sigma}^2), \quad (30)$$

where  $\kappa$  is the added normal Gaussian noise and  $a_{\text{Low}} = -\pi$ ,  $a_{\text{High}} = +\pi$  are the lower and upper limit value for the selected action that is clipped to ensure a feasible action which may not be in the determined interval due to added noise. Also, the constant  $c$  truncates the added noise at inner stage to keep the target action close to the original action.

The detailed description of the TD3 is given in Algorithm 1. A central controller at the BS is collecting and processing the required information for the algorithm execution. First, the six DNNs are initialized by their parameter weights, i.e., the actor network  $\xi^{\text{act}}$ , the critic networks  $\xi_i^{\text{crit}}$ ,  $i \in \{1, 2\}$  coefficients are initialized randomly while the target actor and critic networks' parameters are determined by replicating the primary actor and critic networks' coefficients, respectively. Also, the empty experience replay memory with specified capacity is prepared and the discount factor  $\gamma$ , learning rates, soft update hyperparameter  $\tau$ , maximum step size  $N_{\text{steps}}$  and episodes  $N_{\text{episode}}$  are determined. In the training stage, the reflective phase matrix at the RIS is randomly initialized. The current CSI of the actuators which contains the effective channels' coefficients is acquired and the state set is formed, correspondingly. Next, the action, i.e., the phase shift matrix is collected from the output of the actor DNN with parameter set  $\xi^{\text{act}}$  by importing the current state vector as the input. Next, the observed reward, taken action, the current state  $s$ , and the next state  $s'$ , i.e., the modified channels' coefficients in terms of the phase shift values given by the actor network are recorded at the experience replay buffer. To

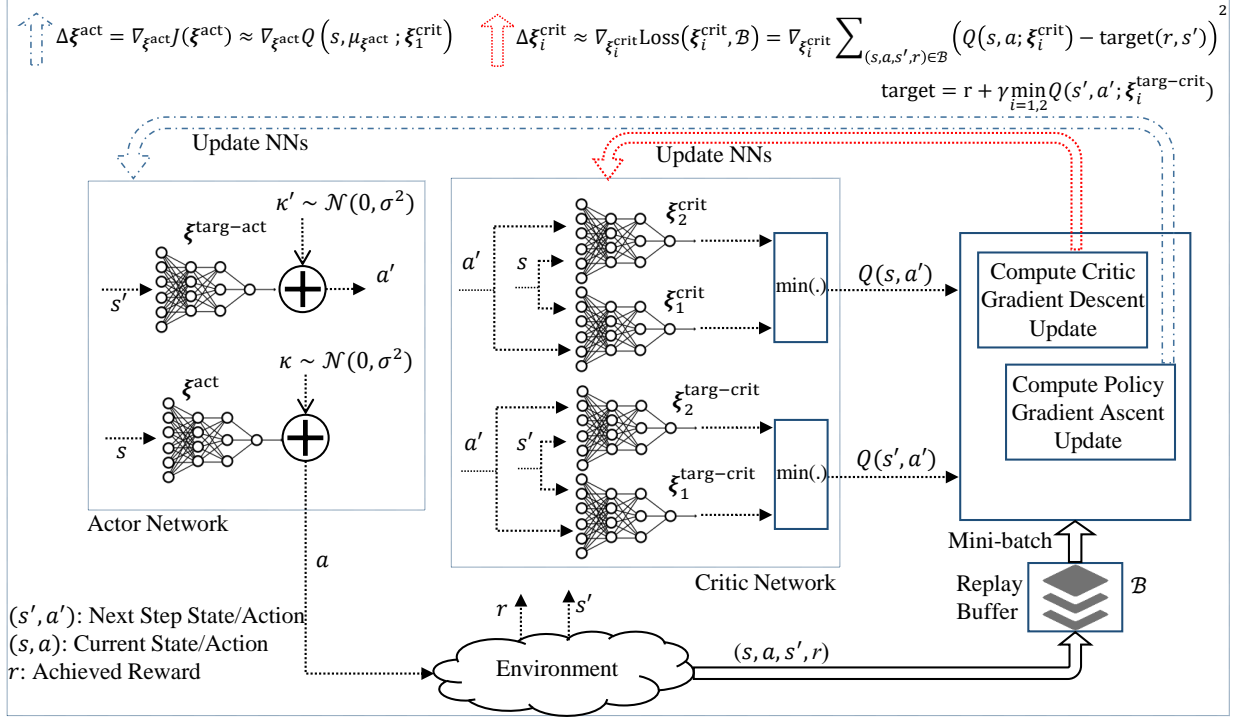


Fig. 2: The agent diagram of TD3 method.

update the DNNs, a mini-batch of stored experience memory is randomly selected, then, the target actions are computed via target actor DNN with weights  $\xi^{\text{targ-act}}$  and the target values are evaluated by selecting the minimum value of target critic DNNs' output which correspond to minimizing the loss function by performing gradient descent method. In addition, when it is time to update the actor and target networks, e.g., out of  $t'$  steps where typically  $t' = 2$  (once in every two steps), the gradient ascent is employed to compute the new coefficients of DNNs, i.e., renewal of  $\xi^{\text{targ-act}}$ ,  $\xi^{\text{targ-crit}}$ , and  $\xi^{\text{act}}$ .

### C. Applying TD3 to Solve **P1**

A preliminary step to solve the problem **P1** with TD3 is to map the components and properly define the algorithm states, actions and the reward function. In this section, we investigate them in detail as follows:

1) *States*: The agent interacts with the environment to optimize the FBL rate performance while ensuring a target BLER. Hence, the agent only has knowledge about the local information, e.g., the channels' response. Consequently, the DRL agent state space is defined as the

---

**Algorithm 1: Twin Delayed DDPG (TD3) Algorithm**


---

**Input:** The number of actuators, the RIS amplitude-phase response model, position of the BS and actuators in 2D-plane.

**Output:** Trained agent with DNNs' weight coefficients.

```

1 Initialization: Initial values for weights  $\xi^{\text{act}}$ ,  $\xi_1^{\text{crit}}$  and  $\xi_2^{\text{crit}}$ , empty replay memory  $\mathcal{B}$ . Let
    $\xi^{\text{targ-act}} \leftarrow \xi^{\text{act}}$ ,  $\xi_1^{\text{targ-crit}} \leftarrow \xi_1^{\text{crit}}$  and  $\xi_2^{\text{targ-crit}} \leftarrow \xi_2^{\text{crit}}$ , soft update coefficient  $\tau$ , the discount
   factor  $\gamma$ , the learning rates, the maximum steps  $N_{\text{steps}}$ , and maximum episodes  $N_{\text{episode}}$ ;
2 for  $e = 1, 2, \dots, N_{\text{episode}}$  do
3   Randomly initiate the phase matrix at the RIS;
4   for  $t = 1, 2, \dots, N_{\text{steps}}$  do
5     Obtain current CSI  $\{\mathbf{h}_1(t), \mathbf{h}_2(t), \dots, \mathbf{h}_K(t)\}$ ;
6     Select action  $a = \text{clip}(\mu(s; \xi^{\text{act}}) + \kappa, a_{\text{Low}}, a_{\text{High}})$ , where  $\kappa \sim \mathcal{N}(0, \sigma^2)$ ;
7     Perform the action  $a$  selected above;
8     Observe next state  $s'$  and the reward value  $r$ ;
9     Store the tuple  $(s, a, s', r)$  in the replay memory  $\mathcal{B}$ ;
10    Sample a batch of tuple  $\mathbb{B} \subset \mathcal{B}$  from experience replay memory;
11    Compute target actions given as
           
$$a' = \text{clip}(\mu(s'; \xi^{\text{targ-act}}) + \text{clip}(\kappa, -c, +c), a_{\text{Low}}, a_{\text{High}}), \kappa \sim \mathcal{N}(0, \tilde{\sigma}^2)$$

12    Compute the target value,  $\text{target}(r, s') = r + \gamma \min_{i \in \{1, 2\}} Q(s', a'; \xi_i^{\text{targ-crit}})$ ;
13    Update the critic networks by performing gradient descent using
           
$$\frac{1}{|\mathbb{B}|} \nabla_{\xi_i^{\text{crit}}} \sum_{(s, a, s', r) \in \mathbb{B}} (Q(s, a; \xi_i^{\text{crit}}) - \text{target}(r, s'))^2, \text{ for } i \in \{1, 2\}.$$

14    if time to update policy network then
15      Update the policy network by performing gradient ascent with
           
$$\frac{1}{|\mathbb{B}|} \nabla_{\xi^{\text{act}}} \sum_{s \in \mathbb{B}} Q(s, a = \mu(s; \xi^{\text{act}}); \xi_1^{\text{crit}}),$$

16      Update the target networks with
           
$$\begin{aligned} \xi^{\text{targ-act}} &\leftarrow \tau \xi^{\text{act}} + (1 - \tau) \xi^{\text{targ-act}}, \\ \xi_i^{\text{targ-crit}} &\leftarrow \tau \xi_i^{\text{crit}} + (1 - \tau) \xi_i^{\text{targ-crit}}, \text{ for } i \in \{1, 2\}. \end{aligned}$$

17    end
18  end
19 end

```

---

aggregation of the real and imaginary parts of the total channel coefficients  $(\mathbf{h}_k, \forall k)$ . In other words, we have

$$s_t = \{\mathbf{h}_1(t), \mathbf{h}_2(t), \dots, \mathbf{h}_K(t)\}, \quad (31)$$

2) *Actions*: The action is determined as the value of phase shift at each element ( $\theta_n(t), \forall n$ ) and the action set in time  $t$  is given by

$$a_t = \{\theta_1(t), \theta_2(t), \dots, \theta_K(t)\}, \quad (32)$$

such that each element value is chosen from the interval  $\theta_n(t) \in [-\pi, \pi], \forall n$ .

3) *Reward Function*: The objective function in **P1** is considered as the step-reward function which is to be maximized over time-steps  $t$ , i.e.,  $L_{\text{tot}}(\Theta)$ .

#### D. Complexity Analysis

In this section, we discuss the computational complexity of proposed TD3 to solve the **P1**. Let  $n_L$  be the number of layers in each DNN and  $z_l$  be the number of neurons in layer  $l$ . Then, in the training mode, the evaluation and update in one time-step is  $\mathcal{O}(|\mathbb{B}| \times \sum_{l=1}^{n_L-1} z_l z_{l+1})$  [19] where  $|\mathbb{B}|$  denotes the size of batch tuple. Since the TD3 algorithm has a finite number of DNNs and it takes  $N_{\text{episode}} \times N_{\text{steps}}$  iterations to complete the training phase in which  $N_{\text{steps}}$  is the number of steps in each episode and  $N_{\text{episode}}$  is the total number of episodes. Therefore, the total computational complexity will be  $\mathcal{O}(|\mathbb{B}| N_{\text{episode}} N_{\text{steps}} \sum_{l=1}^{n_L-1} z_l z_{l+1})$ .

## IV. NUMERICAL RESULTS

In this section, we numerically evaluate the considered phase shift optimization problem by using the proposed DRL method. Table II shows the considered parameters selected for the network. We choose a generic channel model to obtain insights about the proposed approach's performance trends independent of the operating frequency and employed channel model. Evaluations under specific channel models, including indoor factory scenarios and millimeter wave channels, is left for future studies. Since, the components and robots in an industrial automation are in almost fixed position, we considered three actuators in a factory environment located in 2D-plane coordinates at  $[90, 70]$ ,  $[70, 90]$  and  $[60, 80]$  where a BS is positioned at  $[75, 75]$  and the RIS is located in the edge side of the factory at  $[150, 150]$ . The large scale path loss for the reflected channels is modeled as  $\text{PL}(\text{dB})_{\text{NLoS}} = 34.53 + 38 \log_{10}(D[\text{m}])$  where  $D$  is the distance between the transmitter and the receiver while the LoS channel path loss coefficient is chosen to be higher due to blockage, i.e.,  $\text{PL}(\text{dB})_{\text{LoS}} = 34.53 + 40 \log_{10}(D[\text{m}])$ . The Monte Carlo simulation results are averaged over 200 realization of channel's random components. The non-linear amplitude response and the quantized value at the RIS phase shift element is illustrated

TABLE II: Simulation parameters.

Parameter	Default value
Number of actuators ( $K$ )	3
Number of BS antennas ( $M$ )	4
Number of RIS elements ( $N$ )	25
Rician factors ( $\zeta$ and $\zeta_k^{\text{RIS}} \forall k$ )	10
BS transmit power	20 mW
Target error probability ( $\varepsilon_k^{\text{th}}, \forall k$ )	$10^{-7}$
$f_d T_d T_s$	0.1
Outdated CSI coefficient ( $\rho_d$ )	0.9
Receiver noise figure (NF)	3 dB
Noise power density ( $N_0$ )	-174 dBm/Hz
Channel blocklength ( $M$ )	20
Bandwidth ( $W$ )	20 MHz
Carrier frequency	1900 MHz
BS height	12.5 m
BS location in 2D plane	[75, 75] m
RIS position in 2D plane	[150, 150] m
	$\beta_{\min} = 0.6$
RIS phase shifter parameters	$\alpha = 1.6$
	$\phi = 0.43\pi$

in Fig. 3a along with the quantization input-output diagram for 2-bit and 3-bit quantizers in Fig. 3b.

The learning rate in actor networks of TD3 agent is set to  $10^{-4}$  and for the critic networks is  $10^{-3}$ . The activation functions in all hidden layers are considered as  $ReLU(\cdot)$  except for the last layer in which for the actor network is assumed to be  $\tanh(\cdot)$  to provide better gradient. The experience replay buffer capacity is 5000 with batch size 32 such that the samples are uniformly selected from the buffer data. The number of steps in an episode is set to 200. Furthermore, the exploration noise in TD3 actor networks which is a zero-mean normal random variable has  $0.1 \times \pi$  standard deviation. The target actor/critic networks' soft update coefficient is  $\tau = 0.005$ . During the updating procedure, the policy network is being updated every two steps.

Fig. 4a illustrates the convergence of a  $N = 20$  element RIS with  $\beta_{\min} = \{0.2, 0.6\}$ . The learning curves show that when the minimum amplitude is lower, it is of paramount importance to optimize the phase shifts at the RIS elements to preserve the performance loss due to amplitude deterioration. We also observe that the learning curves get lower values of rates at the beginning episodes. This is because the agent needs to try many possibilities in order to find the optimal policy so as to maximize the expected reward which is the network sum achievable rate. Once,

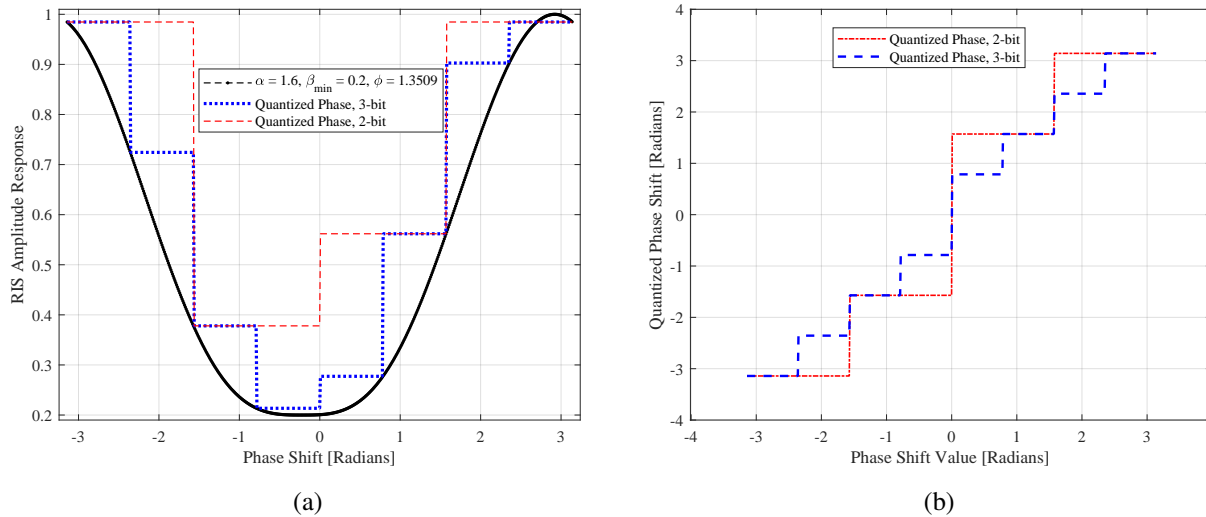


Fig. 3: (a): Non-linear RIS amplitude response versus phase shift values. (b): Quantizer diagram.

the DNNs begin learning the environment model, the curves start to go higher. Fig. 4b shows the convergence behavior of the proposed phase shift design problem in terms of different learning rates of the actor network. It can be perceived that the total rate increases as training continues which demonstrates the effectiveness of the TD3 method in solving **P1**. Also, it is observed that when the learning rate is lower, the actor network suggests actions, i.e., phase shift values that can reduce the system performance in the beginning episodes. In addition, as the learning rate goes higher, the reward converges quickly. Consequently, the learning rates are sensitive to the convergence rate that should be appropriately selected.

In Fig. 5 the average FBL rate for continuous phase shift control is illustrated for TD3 and DDPG methods. The curves plot the mean and standard deviation of the FBL rate throughout episodes while filling the space between the positive and negative mean error using a semi-transparent background. As observed, the TD3 has fewer fluctuations in terms of the FBL rate compared to the DDPG algorithm which is shown as shaded region around the curves. In addition, TD3 outperforms DDPG method in both final performance and learning speed in phase control. This observation highlights the applicability of proposed TD3 algorithm in phase matrix optimization of RIS-aided networks toward realizing reliable and robust wireless links over short packet communications.

On the other side, Fig. 6 shows the target BLER performance in terms of averaged total FBL rate with  $N = 25$  reflective elements. In addition, the BLER deterioration due to rate

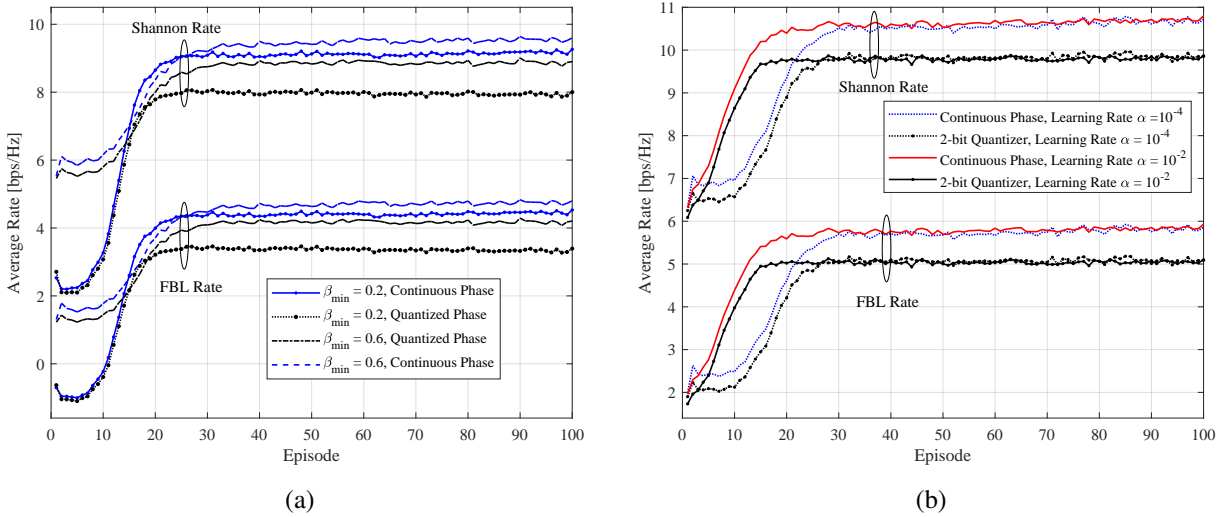


Fig. 4: (a): The comparison of the algorithm convergence in terms of different minimum amplitudes for the non-ideal RIS ( $N = 20$ ). (b): The convergence illustration of the TD3 approach.

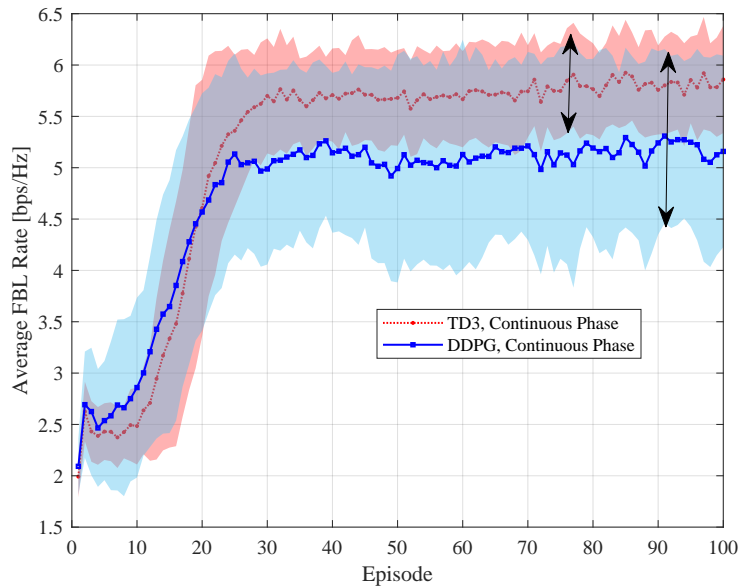


Fig. 5: Comparison of TD3 and DDPG convergence for similar DNN configurations and parameters. Note the fluctuations in DDPG method which has occurred due to frequent policy network updates.

increase or leveraging 2-bit quantizer is illustrated. From Fig. 6 it is inferred that the BLER worsening due to either using a 2-bit quantizer or increasing the transmission rate, is noticeable and highlighted even more. For instance, when the target BLER is set to  $10^{-9}$ , the achievable

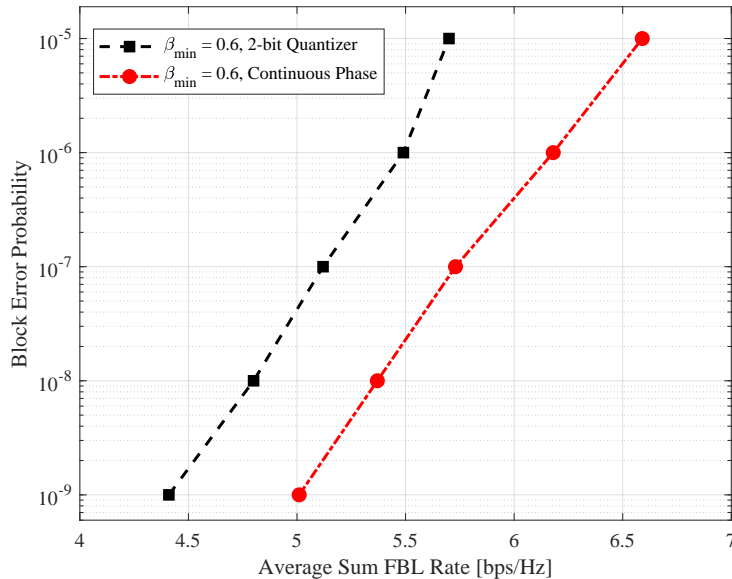


Fig. 6: The block error probability in terms of averaged total FBL rate in continuous and quantized phase shift.

FBL rate will be around 5 bps/Hz, however, when the 2-bit quantizer is exploited, the target BLER will be increased to  $10^{-7}$  which might have a significant impact on the system reliability performance. This observation highlights the sensitivity of design considerations in industrial automation systems where establishing an ultra-reliable link is of paramount importance.

Fig. 7 shows the impact of increasing the transmit power of BS on the average achievable rates. As it is highlighted in the curves, the uppermost red curves show the case that the RIS is ideal and the phase shifts are being allocated continuously without quantization. It is observed that increasing the transmit power of the BS achieves a higher total rate in the system. On the other side, the performance of the system with non-ideal RIS and with quantization process is illustrated in the lowermost black curves. This shows that the actual system achievable rate whether in the Shannon or FBL regime will fall into these two extreme points which highlights the applicability of our proposed resource allocation algorithm in system-level design considerations to establish reliable communications in industrial environments.

Similarly, in Fig. 8 the network sum rate is assessed in terms of increasing the total number of reflective elements at the RIS. A gap is also observed between the upperbound performance and lowerbound case which demonstrates that the system actual performance will lie between these two curves. Another result from these curves, is that the total achievable rate in all cases increases

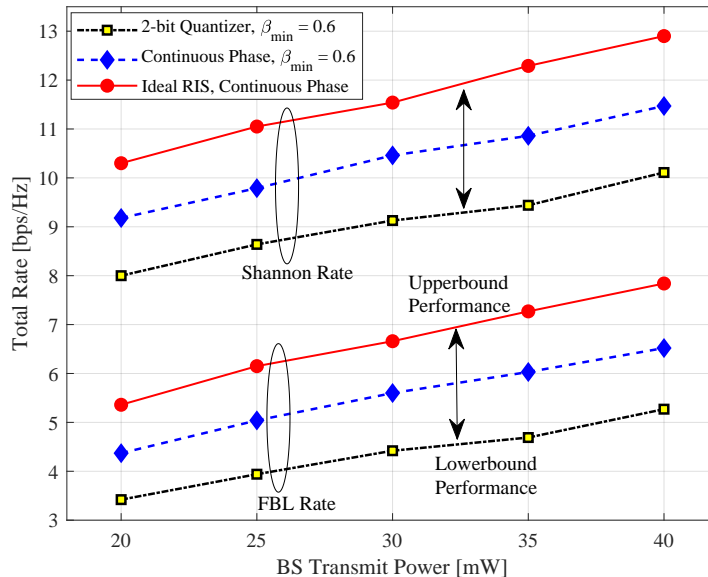


Fig. 7: The impact of increasing the transmit power of BS to the converged average rate in FBL and Shannon regime. Note the gap between the upperbound and lowerbound curves.

with the number of RIS elements, i.e., with/without ideal/non-ideal RIS or with quantized phase shifts. The similar performance is also shown in FBL and Shannon rates. On the other hand, the slope of the curves are quite similar when the number of RIS elements start to increase which additionally shows the practicality of the proposed TD3 algorithm in ideal/non-ideal reflective phase shift design problems.

Fig. 9 shows the impact of total system rate with/without the presence of the LoS link for different number of quantization bits at the RIS phase shift elements. It is observed that when the actuator loses the LoS connection due to possible blockages in the factory, the system FBL rate reduces rather slightly. In addition, with a higher minimum amplitude value, i.e.,  $\beta_{\min}$  at the RIS, the system performance loss can be compensated to preserve the rate loss. Also, one may increase the total rate by adopting higher quantization bits at the RIS processing elements. Nevertheless, the impact of minimum amplitude on increasing the total rate is comparable to when the number of quantization bits increases.

## V. CONCLUSION

In this paper, we have studied the reflective phase shift design problem by a novel and efficient DRL algorithm in practical RIS-aided URLLC systems over short packet communications with

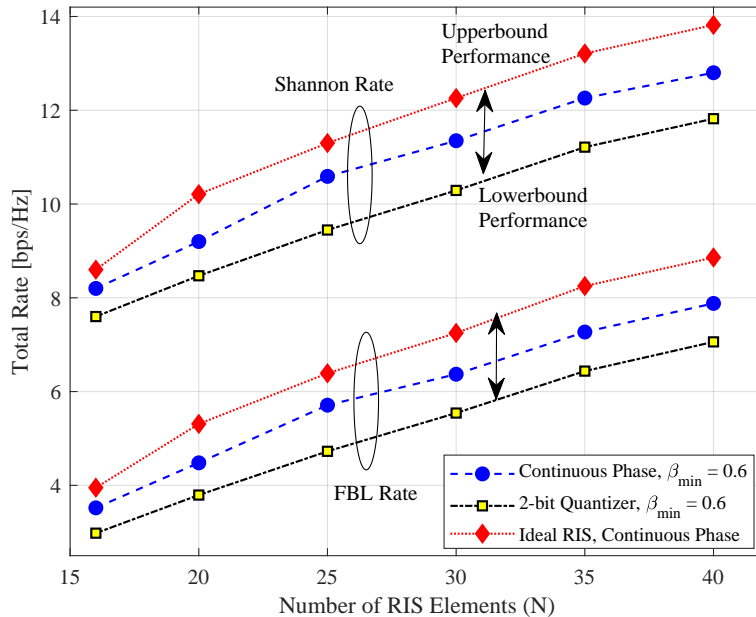


Fig. 8: The effect of increasing number of the RIS elements on the total achievable rate of the system. Note the gap between the upperbound and lowerbound curves.

impairments that are modeled in terms of the amplitude response by changing the phase shift values. First, the problem framework with the objective of maximizing total FBL rate while meeting a given target reliability of actuators in a factory environment is proposed where the constraints are the elements' amplitude response in terms of phase shift and the discrete selection of each phase value due to quantization process. Moreover, the channel coefficients' uncertainty due to transmission and processing delay which leads to feedback delay is taken into account in the proposed formulations. Since the proposed problem has highly non-linear constraints due to considering practical phase shift response, it is more challenging to solve via optimization-based algorithms that are usually computationally inefficient even in ideal scenarios. Thus, we have introduced a policy gradient DRL algorithm based on unsupervised actor-critic methods to optimize the phase shifts which concurrently learns a Q-function and a policy. The utilized DRL method, i.e., TD3 has addressed the issues in the conventional DDPG method that dramatically overestimate action-value function, which then leads to the policy breaking. Therefore, the novel TD3 algorithm is leveraged to tackle the problem. The numerical results demonstrate the applicability of the proposed DRL method in practical RIS phase shift design problems in time-sensitive applications that exploit short packets in URLLC systems by two-fold

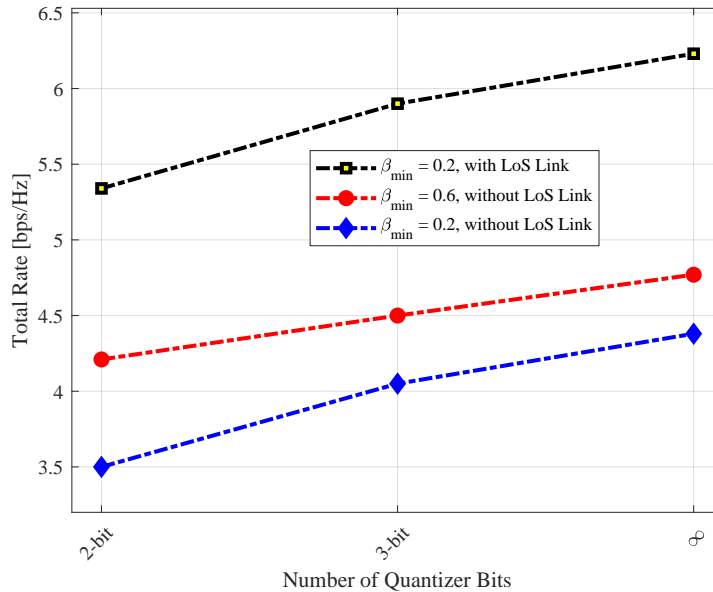


Fig. 9: The impact of the minimum RIS amplitude  $\beta_{\min}$  on the achievable rates with 2-bit, 3-bit quantizer and continuous phase shifts.

improvement in total achieved FBL rate compared to random phase shift design.

## REFERENCES

- [1] N. H. Mahmood, S. Böcker, A. Munari, F. Clazzer, I. Moerman *et al.*, *White paper on critical and massive machine type communication towards 6G*, ser. 6G Research Visions, nr. 11, N. H. Mahmood, O. Lopez, O.-S. Park, I. Moerman, K. Mikhaylov *et al.*, Eds. Oulu, Finland: University of Oulu, Jun. 2020. [Online]. Available: <http://jultika.oulu.fi/files/isbn9789526226781.pdf>
- [2] G. Aceto, V. Persico, and A. Pescapé, “A survey on information and communication technologies for Industry 4.0: State-of-the-art, taxonomies, perspectives, and challenges,” *IEEE Commun. Surv. Tutorials*, vol. 21, no. 4, pp. 3467–3501, Oct. 2019.
- [3] N. H. Mahmood, O. A. Lopez, H. Alves, and M. Latva-Aho, “A predictive interference management algorithm for URLLC in beyond 5G networks,” *IEEE Commun. Lett.*, vol. 25, no. 3, pp. 995–999, Mar. 2021.
- [4] P. Popovski, C. Stefanovic, J. J. Nielsen, E. de Carvalho, M. Angjelichinoski *et al.*, “Wireless access in ultra-reliable low-latency communication (URLLC),” *IEEE Trans. Commun.*, vol. 67, no. 8, pp. 5783–5801, May 2019.
- [5] Y. Polyanskiy, H. V. Poor, and S. Verdú, “Channel coding rate in the finite blocklength regime,” *IEEE Trans. Inf. Theory*, vol. 56, no. 5, pp. 2307–2359, May 2010.
- [6] M. Di Renzo, A. Zappone, M. Debbah, M.-S. Alouini, C. Yuen *et al.*, “Smart radio environments empowered by reconfigurable intelligent surfaces: How it works, state of research, and road ahead,” *IEEE J. Sel. Areas Commun.*, Apr. 2020.
- [7] R. Hashemi, S. Ali, N. H. Mahmood, and M. Latva-aho, “Average rate and error probability analysis in short packet communications over RIS-aided URLLC systems,” *IEEE Trans. Veh. Technol.*, vol. 70, no. 10, pp. 10 320–10 334, 2021.

- [8] —, “Average rate analysis of RIS-aided short packet communication in URLLC systems,” in *Proc. IEEE Int. Conf. Commun. Work. (ICC Work.)*, Montreal, QC, Canada, 2021, pp. 1–6.
- [9] Q. Wu and R. Zhang, “Beamforming optimization for wireless network aided by intelligent reflecting surface with discrete phase shifts,” *IEEE Trans. Commun.*, vol. 68, no. 3, pp. 1838–1851, Mar. 2020.
- [10] S. Abeywickrama, R. Zhang, Q. Wu, and C. Yuen, “Intelligent reflecting surface: Practical phase shift model and beamforming optimization,” *IEEE Trans. Commun.*, vol. 68, no. 9, pp. 5849–5863, Sep. 2020.
- [11] S. Ali, W. Saad, N. Rajatheva, K. Chang, D. Steinbach *et al.*, “6G white paper on machine learning in wireless communication networks,” Apr. 2020. [Online]. Available: <http://arxiv.org/abs/2004.13875>
- [12] S. Ali, N. Rajatheva, and W. Saad, “Fast uplink grant for machine type communications: Challenges and opportunities,” *IEEE Commun. Mag.*, vol. 57, no. 3, pp. 97–103, 2019.
- [13] M. Bennis, M. Debbah, and H. V. Poor, “Ultra-reliable and low-latency wireless communication: Tail, risk, and scale,” *Proc. IEEE*, vol. 106, no. 10, pp. 1834–1853, 2018.
- [14] W. R. Ghanem, V. Jamali, and R. Schober, “Joint beamforming and phase shift optimization for multicell IRS-aided OFDMA-URLLC systems,” in *Proc. IEEE Wireless Commun. and Networking Conf.*, Nanjing, China, 2021, pp. 1–7.
- [15] A. Ranjha and G. Kaddoum, “URLLC facilitated by mobile UAV relay and RIS: A joint design of passive beamforming, blocklength and UAV positioning,” *IEEE Internet Things J.*, vol. 8, no. 6, pp. 4618–4627, 2021.
- [16] H. Xie, J. Xu, Y.-F. Liu, L. Liu, and D. W. K. Ng, “User grouping and reflective beamforming for IRS-aided URLLC,” *IEEE Wireless Commun. Lett.*, pp. 1–1, 2021.
- [17] M. Almekhlafi, M. A. Arfaoui, M. Elhattab, C. Assi, and A. Ghayeb, “Joint scheduling of eMBB and URLLC services in RIS-aided downlink cellular networks,” in *Proc. IEEE Int. Conf. Comput. Commun. Netw. (ICCCN)*, Athens, Greece, Jul. 2021, pp. 1–9.
- [18] M. AL-Mekhlafi, M. A. Arfaoui, M. Elhattab, C. Assi, and A. Ghayeb, “Joint resource allocation and phase shift optimization for RIS-aided eMBB/URLLC traffic multiplexing,” Aug. 2021. [Online]. Available: <https://arxiv.org/abs/2108.02346v1>
- [19] H. Yang, Z. Xiong, J. Zhao, D. Niyato, L. Xiao *et al.*, “Deep reinforcement learning-based intelligent reflecting surface for secure wireless communications,” *IEEE Trans. Wireless Commun.*, vol. 20, no. 1, pp. 375–388, Jan. 2021.
- [20] X. Liu, Y. Liu, and Y. Chen, “Machine learning empowered trajectory and passive beamforming design in UAV-RIS wireless networks,” *IEEE J. Sel. Areas Commun.*, vol. 39, no. 7, pp. 2042–2055, 2020.
- [21] K. Feng, Q. Wang, X. Li, and C. K. Wen, “Deep reinforcement learning based intelligent reflecting surface optimization for MISO communication systems,” *IEEE Wireless Commun. Lett.*, vol. 9, no. 5, pp. 745–749, May 2020.
- [22] A. Faisal, I. Al-Nahhal, O. A. Dobre, and T. M. N. Ngatched, “Deep reinforcement learning for optimizing RIS-assisted HD-FD wireless systems,” *IEEE Commun. Lett.*, pp. 1–1, 2021.
- [23] C. Huang, G. Chen, Y. Gong, M. Wen, and J. A. Chambers, “Deep reinforcement learning based relay selection in intelligent reflecting surface assisted cooperative networks,” *IEEE Wireless Commun. Lett.*, vol. 10, no. 5, pp. 1036–1040, Feb. 2021.
- [24] C. Huang, Z. Yang, G. C. Alexandropoulos, K. Xiong, L. Wei *et al.*, “Hybrid beamforming for RIS-empowered multi-hop terahertz communications: A DRL-based method,” in *Proc. IEEE Global Telecommun. Conf. Work.*, Taipei, Taiwan, Dec. 2020, pp. 1–6.
- [25] —, “Multi-hop RIS-empowered terahertz communications: A DRL-based hybrid beamforming design,” *IEEE J. Sel. Areas Commun.*, vol. 39, no. 6, pp. 1663–1677, Jun. 2021.
- [26] C. Huang, R. Mo, and C. Yuen, “Reconfigurable intelligent surface assisted multiuser MISO systems exploiting deep reinforcement learning,” *IEEE J. Sel. Areas Commun.*, vol. 38, no. 8, pp. 1839–1850, Aug. 2020.

- [27] G. Lee, M. Jung, A. T. Z. Kasgari, W. Saad, and M. Bennis, "Deep reinforcement learning for energy-efficient networking with reconfigurable intelligent surfaces," in *Proc. IEEE Int. Conf. Commun.*, Dublin, Ireland, Jun. 2020.
- [28] J. Lin, Y. Zout, X. Dong, S. Gong, D. T. Hoang *et al.*, "Deep reinforcement learning for robust beamforming in IRS-assisted wireless communications," in *Proc. IEEE Global Telecommun. Conf.*, Taipei, Taiwan, Dec. 2020, pp. 1–6.
- [29] Z. Yang, Y. Liu, Y. Chen, and N. Al-Dhahir, "Machine learning for user partitioning and phase shifters design in RIS-aided NOMA networks," *IEEE Trans. Commun.*, pp. 1–1, 2021.
- [30] M. Shehab, B. S. Ciftler, T. Khattab, M. Abdallah, and D. Trinchero, "Deep reinforcement learning powered IRS-assisted downlink NOMA," Apr. 2021. [Online]. Available: <http://arxiv.org/abs/2104.01414>
- [31] A. Feriani, A. Mezghani, and E. Hossain, "On the robustness of deep reinforcement learning in IRS-aided wireless communications systems," Jul. 2021. [Online]. Available: <https://arxiv.org/abs/2107.08293v2>
- [32] H. Yang, Z. Xiong, J. Zhao, D. Niyato, Q. Wu *et al.*, "Intelligent reflecting surface assisted anti-jamming communications: A fast reinforcement learning approach," *IEEE Trans. Wireless Commun.*, vol. 20, no. 3, pp. 1963–1974, Mar. 2021.
- [33] X. Guo, Y. Chen, and Y. Wang, "Learning-based robust and secure transmission for reconfigurable intelligent surface aided millimeter wave UAV communications," *IEEE Wireless Commun. Lett.*, vol. 10, no. 8, pp. 1795–1799, 2021.
- [34] K. K. Nguyen, S. Khosravirad, L. D. Nguyen, T. T. Nguyen, and T. Q. Duong, "Intelligent reconfigurable surface-assisted multi-UAV networks: Efficient resource allocation with deep reinforcement learning," May 2021. [Online]. Available: <http://arxiv.org/abs/2105.14142>
- [35] S. Jiao, X. Xie, and Z. Ding, "Deep reinforcement learning based optimization for IRS based UAV-NOMA downlink networks," Jun. 2021. [Online]. Available: <http://arxiv.org/abs/2106.09616>
- [36] S. Fujimoto, H. Hoof, and D. Meger, "Addressing function approximation error in actor-critic methods," in *Proc. Int. Conf. Mach. Learn. ICML*. Stockholm, Sweden: PMLR, 2018, pp. 1587–1596.
- [37] Y. Jia, C. Ye, and Y. Cui, "Analysis and optimization of an intelligent reflecting surface-assisted system with interference," *IEEE Trans. Wireless Commun.*, vol. 19, no. 12, pp. 8068–8082, 2020.
- [38] N. H. Mahmood, N. Pratas, T. H. Jacobsen, and P. E. Mogensen, "On the performance of one stage massive random access protocols in 5G systems," in *Proc. 9th International Symposium on Turbo Codes and Iterative Information Processing, (ISTC)*, Brest, France, Sep. 2016, pp. 340–344.
- [39] A. Anand and G. De Veciana, "Resource allocation and HARQ optimization for urllc traffic in 5G wireless networks," *IEEE J. Sel. Areas Commun.*, vol. 36, no. 11, pp. 2411–2421, Nov. 2018.
- [40] J. Sachs, G. Wikstrom, T. Dudda, R. Baldemair, and K. Kittichokechai, "5G radio network design for ultra-reliable low-latency communication," *IEEE Netw.*, vol. 32, no. 2, pp. 24–31, 2018.
- [41] P. Popovski, J. J. Nielsen, C. Stefanovic, E. d. Carvalho, E. Strom *et al.*, "Wireless access for ultra-reliable low-latency communication: Principles and building blocks," *IEEE Netw.*, vol. 32, no. 2, pp. 16–23, Mar. 2018.
- [42] A. Avranas, M. Kountouris, and P. Ciblat, "Energy-latency tradeoff in ultra-reliable low-latency communication with retransmissions," *IEEE J. Sel. Areas Commun.*, vol. 36, no. 11, pp. 2475–2485, 2018.
- [43] Y. Huang, F. Al-Qahtani, C. Zhong, Q. Wu, J. Wang *et al.*, "Performance analysis of multiuser multiple antenna relaying networks with co-channel interference and feedback delay," *IEEE Trans. Commun.*, vol. 62, no. 1, pp. 59–73, 2014.
- [44] C. Szepesvári, "Algorithms for reinforcement learning," *Synthesis lectures on artificial intelligence and machine learning*, vol. 4, no. 1, pp. 1–103, 2010.
- [45] R. S. Sutton and A. G. Barto, *Reinforcement learning: An introduction*. MIT press, 2018.
- [46] T. P. Lillicrap, J. J. Hunt, A. Pritzel, N. Heess, T. Erez *et al.*, "Continuous control with deep reinforcement learning," *arXiv preprint arXiv:1509.02971*, 2015.